

# A COMPARATIVE EVALUATION OF THE POTENTIAL OF CLOSE RANGE PHOTOGRAMMETRIC TECHNIQUE FOR THE 3D MEASUREMENT OF THE BODY OF A NISSAN PATROL CAR

E.G. Parmehr, A. Azizi

Dept. of Geomatics and Surveying Engineering, Faculty of Engineering,  
University of Tehran, 11365/4563 Tehran, Iran.  
[parmehr@ut.ac.ir](mailto:parmehr@ut.ac.ir), [aazizi@ut.ac.ir](mailto:aazizi@ut.ac.ir)

Commission V, WG VI/1

**KEY WORDS:** Close Range Photogrammetry, Industry, Metric Camera, Design, Calibration, Measurement, Accuracy.

## ABSTRACT:

Close range photogrammetry as applied for the as-built and as designed comparisons in the car industry has attracted serious attentions in recent years. This thesis reports in some details an off-line close range photogrammetric approach for the accurate measurement of the body of a Nissan Patrol car. The photographs are taken by the Zeiss UMK 10/1318U metric camera. In the first stage of the project, the body of the car is marked with the circular shape targets. The object coordinates of these targets were then determined with respect to an arbitrary coordinate system using geodetic surveying technique. In the subsequent stage a network was designed around the Nissan Patrol to be used for installing the cameras. The image coordinates of the target points were then measured by the SD2000 analytical plotter. The object coordinates of these points were calculated using collinearity condition equations combined with various self calibration strategies proposed by: Brown 1975, Brown 1976, Ebner 1976, Moniwa 1977 and El-Hakim 1977. The discrepancies between the coordinates of the points generated by the photogrammetric method and the coordinates of the same points produced by the geodetic approach, is taken as the accuracy criteria. The best results obtained for check points are 0.21 mm (rmse).

## 1. INTRODUCTION

In recent years close range photogrammetry has demonstrated its capability as a powerful technique for the metric acquisition of industrial objects. The close range photogrammetric method reigns supreme as regards the ease of data acquisition, instantaneous data capture and cost effectiveness as compared to alternative solutions. As far as the accuracy of the extracted metric information is concerned, two solutions are common. The first approach employs a non metric camera and compensates the accuracy loss with appropriate mathematical models. The second method on the other hand utilizes a combination of hardware and software solutions by utilizing a metric camera. In this project the second solution is adopted for the measurement of distinct points on a Patrol car using a Zeiss UMK metric camera. Since the internal geometry of this camera is known with sufficient accuracy, no pre-calibration is required. This paper gives a brief outline of the procedures involved in the 3D object coordinates extraction of series of signalized points installed on a Patrol car. The accuracy results are also reported.

## 2. DATA ACQUISITION

The data acquisition stage is briefly outlined in the sub-sections that follow.

### 2.1 UMK 10/1318U metric camera

Image acquisition is conducted with a Zeiss UMK 10/1318U metric camera. This camera has a stable internal geometry with a minimum of lens distortion. The internal geometry is accurately determined by the manufacturer and reported in the

camera documentation. The full camera specification is given in Table 1.

Lens	Lamegon 8/100 B
Focal length	99 mm
Focusing range	1.4 m to infinity
Effective frame size	120 x 166 mm
Camera weight with accessories	20 kg
Effective size of the angular view	79 and 61 degrees for the horizontal and vertical direction

Table 1. UMK 10/1318U camera specifications

### 2.2 Film characteristics

To perform the image acquisition with highest possible resolution, a slow speed film with the finest granularity available in the market was purchased. Since the object being photographed was completely stationary, no motion blur was introduced into the acquired image. Figure 1 and 2 demonstrate the resolution of the selected film as compared with a faster film.

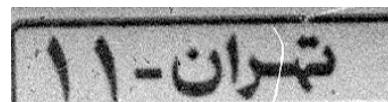


Figure 1. Image of a portion of an object taken by slow film



Figure 2. Image of a portion of an object taken by fast film

### 2.3 Signalized targets

To determine the shape of the signalized target that could be more easily identified and pointed in an image, series of targets with different shapes were designed (Figure 2). These targets were then installed on a surface. Photographs were taken from these targets and the potential of identification and pointing the target centers were experimentally evaluated. The evaluation result indicated that the shapes of the targets are not important as regards the pointing precision. However, amongst the targets that were recorded with a small viewing angle, circular targets indicated better pointing precision. To determine the minimum target size,  $D_m$ , the following relation is adopted:

$$D_{\min} = d \frac{s}{f} \quad (1)$$

where  $d$  is the diameter of the measuring mark;  $s$  is the camera object distance and  $f$  denotes the camera focal length. With the view to the analysis described above, circular targets with diameters of 2 cm were prepared and installed in appropriate places on the body of the Patrol car (Figure 4). To cover the entire body of the car, 120 targets were used. The overall interval between the adjacent targets was about 40 cm.

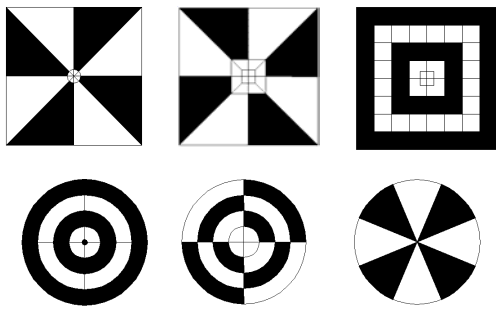


Figure 3. Designed targets



Figure 4. Patrol car and the installed targets

### 2.4 Geodetic network

The 3D object coordinates of the targets with respect to a local geodetic network were determined using the Sokkia Power Set 1000 total station (Figure 4). The accuracy was estimated to be 0.1 mm and 1 second for the distance and angle measurements respectively.

### 2.5 Photogrammetric network

The network for the imaging stations were designed based on the well known  $q$  factor included in the following relation:

$$\bar{\sigma}_c = \frac{q \sigma_i S}{\sqrt{k}} \quad (2)$$

where  $\bar{\sigma}_c$  is the overall accuracy in the object space;  $k$  is the average number of the photographs taken from each station;  $\sigma_i$  denotes the average accuracy of the image point measurement and  $S$  is the average image scale given by:

$$S = \frac{d}{c} \quad (3)$$

where  $c$  is the principal distance of the camera. For a geometrically rigorous photogrammetric network,  $q$  factor is considered to vary from 0.6 to 0.7. By taking into account all constraints for the photogrammetric network design and with several trial and error procedures, the final network presented in Figure 5 was designed.

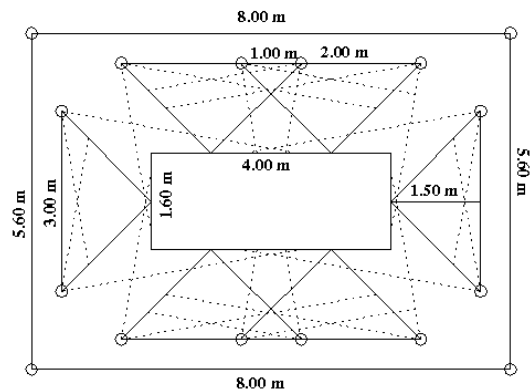


Figure 5. The designed photogrammetric network

### 2.6 Image coordinates measurement

To achieve high accuracy for the image coordinates measurements, Leica SD2000 an analytical plotter is used (Figure 6). The accuracy of the image points measurement were evaluated using a reseau plate. The largest error for the check points on the reseau plate was about 1.75 micrometer using the affine transformation. Figure 7 gives the vector plot of the residual errors.



Figure 6. Leica SD2000 analytical plotter

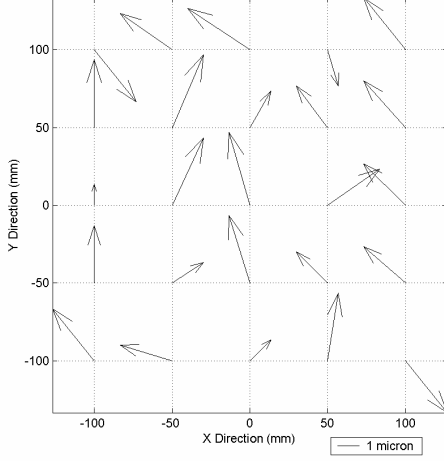


Figure 7. The vector plot of the residual errors for the reseau grid

### 3. COMPUTATION OF THE OBJECT COORDINATE

The approximate values for the camera orientation parameters were calculated using the well known DLT equations given by:

$$x = \frac{L_1 X + L_2 Y + L_3 Z + L_4}{L_9 X + L_{10} Y + L_{11} Z + 1} \quad (4)$$

$$y = \frac{L_5 X + L_6 Y + L_7 Z + L_8}{L_9 X + L_{10} Y + L_{11} Z + 1}$$

Where  $x, y$  are the image coordinates in comparator coordinate system;  $X, Y, Z$  are the corresponding object coordinate and  $L_1, \dots, L_{11}$  are the DLT coefficients. The approximate values for the interior and exterior orientation parameters are given by:

$$\begin{aligned} x_0 &= (L_1 L_9 + L_2 L_{10} + L_3 L_{11}) / (L_9^2 + L_{10}^2 + L_{11}^2) \\ y_0 &= (L_5 L_9 + L_6 L_{10} + L_7 L_{11}) / (L_9^2 + L_{10}^2 + L_{11}^2) \\ c_x &= \sqrt{(L_1^2 + L_2^2 + L_3^2) / (L_9^2 + L_{10}^2 + L_{11}^2) - x_0^2} \\ c_y &= \sqrt{(L_5^2 + L_6^2 + L_7^2) / (L_9^2 + L_{10}^2 + L_{11}^2) - y_0^2} \\ c &= (c_x + c_y) / 2 \end{aligned} \quad (5)$$

$$\begin{aligned} \begin{bmatrix} X_c \\ Y_c \\ Z_c \end{bmatrix} &= - \begin{bmatrix} L_1 & L_2 & L_3 \\ L_5 & L_6 & L_7 \\ L_9 & L_{10} & L_{11} \end{bmatrix}^{-1} \begin{bmatrix} L_4 \\ L_8 \\ 1 \end{bmatrix} \\ \omega &= \tan^{-1}(-L_{10} / L_{11}) \\ \phi &= \sin^{-1} \left( -L_9 / \sqrt{L_9^2 + L_{10}^2 + L_{11}^2} \right) \\ \kappa &= \cos^{-1} \left( (L_1 - x_0 L_9) / (c \cdot \cos \phi \cdot \sqrt{L_9^2 + L_{10}^2 + L_{11}^2}) \right) \end{aligned} \quad (6)$$

As residual systematic errors inevitably remain in the observed data and the conventional approaches for the coordinates refinement can not be entirely eliminated, a self calibration approach is adopted.

$$\begin{aligned} x - x_0 + \Delta x_p &= -c \frac{(X - X_c)m_{11} + (Y - Y_c)m_{12} + (Z - Z_c)m_{13}}{(X - X_c)m_{31} + (Y - Y_c)m_{32} + (Z - Z_c)m_{33}} \\ y - y_0 + \Delta y_p &= -c \frac{(X - X_c)m_{21} + (Y - Y_c)m_{22} + (Z - Z_c)m_{23}}{(X - X_c)m_{31} + (Y - Y_c)m_{32} + (Z - Z_c)m_{33}} \end{aligned} \quad (7)$$

The following additional parameters are implemented for this project:

#### (a) Brown 1975 additional parameters, given by:

$$\begin{aligned} \Delta x_p &= a_1 x + a_2 y + a_3 x^2 + a_4 xy + a_5 y^2 + a_6 x^2 y + a_7 xy^2 \\ &+ \frac{x}{r} (c_1 x^2 + c_2 xy + c_3 y^2 + c_4 x^3 + c_5 x^2 y + c_6 xy^2 + c_7 y^3) \\ &+ x(K_1 r^2 + K_2 r^4 + K_3 r^6) + p_1 (y^2 + 3x^2) + 2p_2 xy + \delta x_p + \left(\frac{x}{c}\right) \delta c \end{aligned} \quad (8)$$

$$\begin{aligned} \Delta y_p &= b_1 x + b_2 y + b_3 x^2 + b_4 xy + b_5 y^2 + b_6 x^2 y + b_7 xy^2 \\ &+ \frac{y}{r} (c_1 x^2 + c_2 xy + c_3 y^2 + c_4 x^3 + c_5 x^2 y + c_6 xy^2 + c_7 y^3) \\ &+ y(K_1 r^2 + K_2 r^4 + K_3 r^6) + 2p_1 xy + p_2 (x^2 + 3y^2) + \delta y_p + \left(\frac{y}{c}\right) \delta c \end{aligned}$$

#### (b) Brown 1976 additional parameters, given by:

$$\begin{aligned} \Delta x_p &= a_1 x + a_2 y + a_3 xy + a_4 y^2 + a_5 x^2 y + a_6 xy^2 + a_7 x^2 y^2 \\ &+ \frac{x}{c} (a_{13} (x^2 - y^2) + a_{14} x^2 y^2 + a_{15} (x^4 - y^4)) \\ &+ x(a_{16} (x^2 + y^2)^2 + a_{17} (x^2 + y^2)^4 + a_{18} (x^2 + y^2)^6) \end{aligned} \quad (9)$$

$$\begin{aligned} \Delta y_p &= a_8 xy + a_9 x^2 + a_{10} x^2 y + a_{11} xy^2 + a_{12} x^2 y^2 \\ &+ \frac{y}{c} (a_{13} (x^2 - y^2) + a_{14} x^2 y^2 + a_{15} (x^4 - y^4)) \\ &+ y(a_{16} (x^2 + y^2)^2 + a_{17} (x^2 + y^2)^4 + a_{18} (x^2 + y^2)^6) \end{aligned}$$

#### (c) Ebner 1976 additional parameters given by:

$$\begin{aligned} \Delta x_p &= a_1 x + a_2 y - a_3 (2x^2 - 4r^2/3) + a_4 xy + a_5 (y^2 - 2r^2/3) \\ &+ a_7 x (y^2 - 2r^2/3) + a_9 y (x^2 - 2r^2/3) + a_{11} (x^2 - 2r^2/3) (y^2 - 2r^2/3) \end{aligned} \quad (10)$$

$$\begin{aligned} \Delta y_p &= -a_1 y + a_2 x + a_3 xy - a_4 (2y^2 - 4r^2/3) + a_6 (x^2 - 2r^2/3) \\ &+ a_8 y (x^2 - 2r^2/3) + a_{10} x (y^2 - 2r^2/3) + a_{12} (x^2 - 2r^2/3) (y^2 - 2r^2/3) \end{aligned}$$

#### (d) El-Hakim 1977 additional parameters given by:

$$\begin{aligned} \Delta x_p &= (x - x_0) T \\ \Delta y_p &= (y - y_0) T \\ T &= a_{00} + a_{11} \cos \lambda + b_{11} \sin \lambda + a_{20} r + a_{22} r \cos^2 \lambda + b_{22} r \sin 2\lambda \\ &+ a_{31} r^2 \cos \lambda + b_{31} r^2 \sin \lambda + a_{33} r^2 \cos 3\lambda + b_{33} r^2 \sin 3\lambda + \dots \end{aligned} \quad (11)$$

$$\lambda = \tan^{-1} \frac{y - y_0}{x - x_0}$$

#### (e) Moniwa 1977 additional parameters given by:

$$\begin{aligned} \Delta x_p &= dr_x + dp_x + dg_x \\ \Delta y_p &= dr_y + dp_y + dg_y \\ dr_x &= (x - x_0) (K_1 r^2 + K_2 r^4 + K_3 r^6) \\ dr_y &= (y - y_0) (K_1 r^2 + K_2 r^4 + K_3 r^6) \\ dp_x &= p_1 (r^2 + 2(x - x_0)^2) + 2p_2 (x - x_0) (y - y_0) \\ dp_y &= p_2 (r^2 + 2(y - y_0)^2) + 2p_1 (x - x_0) (y - y_0) \\ dg_x &= A(x - x_0) \\ dg_y &= B(y - y_0) \end{aligned} \quad (12)$$

#### 4. TEST RESULTS AND COCLUSION REMARKS

The bundle adjustments for all mathematical models given in the preceding section were carried out for 4 convergent photographs (Figure 8). The stability of the solution of the equations were secured using 19 control points of which 11 points appeared in all photographs and hence contributed also as tie points. These tie points played a decisive rule for determination of the self calibration parameters. Figures 9 shows the average accuracies achieved in control and check points for all additional parameters given in the preceding section.



Figure 8. Four convergent photographs

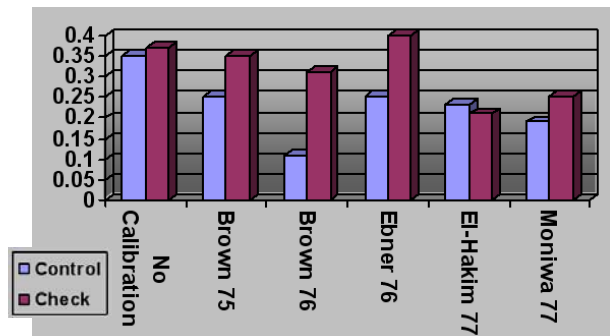


Figure 9. The evaluated overall accuracy in control and check points for all mathematical models

#### 5. REFERENCES

Abdel-Aziz, Y.I., Karara, H.m., 1971. Direct linear transform from comparator coordinate into object-space coordinates. In *ASP Symposium on Close-Range Photogrammetry*. Falls Church, VA: pp.1-18. American Society of Photogrammetry.

Brown, D.C, 1976. The bundle adjustment – progress and prospects. *International Archives of Photogrammetric and Remote Sensing*. Vol. XIII, No. 3. Helsinki.

Ebner, H, 1976. Self calibrating block adjustment. *Bildmessung und Luftbildwesen*, Vol. 4/76.

El-Hakim, S.F, 1977. Compensation of systematic image error using spherical harmonics. *ASP Fall Technical Meeting*, Little Rock.

Fraser, C.S., 1984. Network design consideration for non-topographic photogrammetry. *Photogrammetric Engineering and Remote Sensing*, 50(8): 1115-1126.

Mikhail, E.M., Bethel, J.B and McGlone, J.C., 2001. *Introduction to Modern Photogrammetry*. New York: John Wiley & Sons, Inc.

Moniwa, S.F, 1977. *Advanced photogrammetric system with self-calibration and its applications*. Ph.D. Dissertation, Department of Surveying Engineering, U.N.B., Fredericton.

Slama, C.C., Theurer, C. and Henriksen, S.W., 1980. *Manual of Photogrammetry*. American Society of photogrammetry.